1. Introduction

The focus of the work presented in the initial chapters is to explore the factors that affect the tensile properties of austenitic stainless steels, including the yield strength (or 0.2% proof stress), ultimate tensile strength (UTS) and ductility. Creep can be an important issue when considering elevated temperature applications, but the main aim here is to look at short term properties.

Austenitic stainless steels were invented by Henry Brearley [4], who first used them for aircraft engine exhaust valves in World War One. Today, uses have diverged into power plants and railroad coaches [5]. In 1999, the Victoria Bridge in Brisbane, Australia, had its original carbon steel bearings replaced with type 316 stainless steel, as shown in figure 1.2 [6]. This helped extend the service life of the component, as it is now more resistant to the corrosive nature of tidal waters and pigeon droppings. More recently, Dyson have incorporated austenitic stainless steel into their new twin drum washing machine, *Contrarotator*™ (fig. 1.3) [7]. Their non-magnetic nature also makes them more attractive for implementation into submarine and ship hulls [8]. As they reduce the local disturbance of the Earth's magnetic field, it therefore renders them less detectable to sea mines and enemy vessels.

Stainless steel predominantly contains high levels of chromium and nickel, typically 18Cr-8Ni wt%. Additional elements may be added to enhance performance (fig. 1.1), but the benefits and side effects are sometimes hard to understand. However, various parameters will be examined such as dislocations, stacking faults, grain size, solid solution and precipitation hardening.

1.1 Austenitic Stainless Steel

Corrosion resistance, ductility, good weldability and resistance to high and low operating temperatures [4,9] are some of the many reasons for the use of austenitic steels. Chromium is the main deterrent to corrosion through a process called passivity [10], where chromium combines with oxygen in the atmosphere to form a protective oxide layer [11]. This is especially useful when the metal is scratched, as the oxide layer re-forms quickly, hence protecting it from corrosion. However, chromium is a ferrite stabiliser. To counteract this, nickel is added as an austenite stabiliser, so that the microstructure at ambient temperature is austenitic. Figure 1.4 [12] illustrates the region where stable austenite forms within a pure Fe-18Cr wt% alloy.

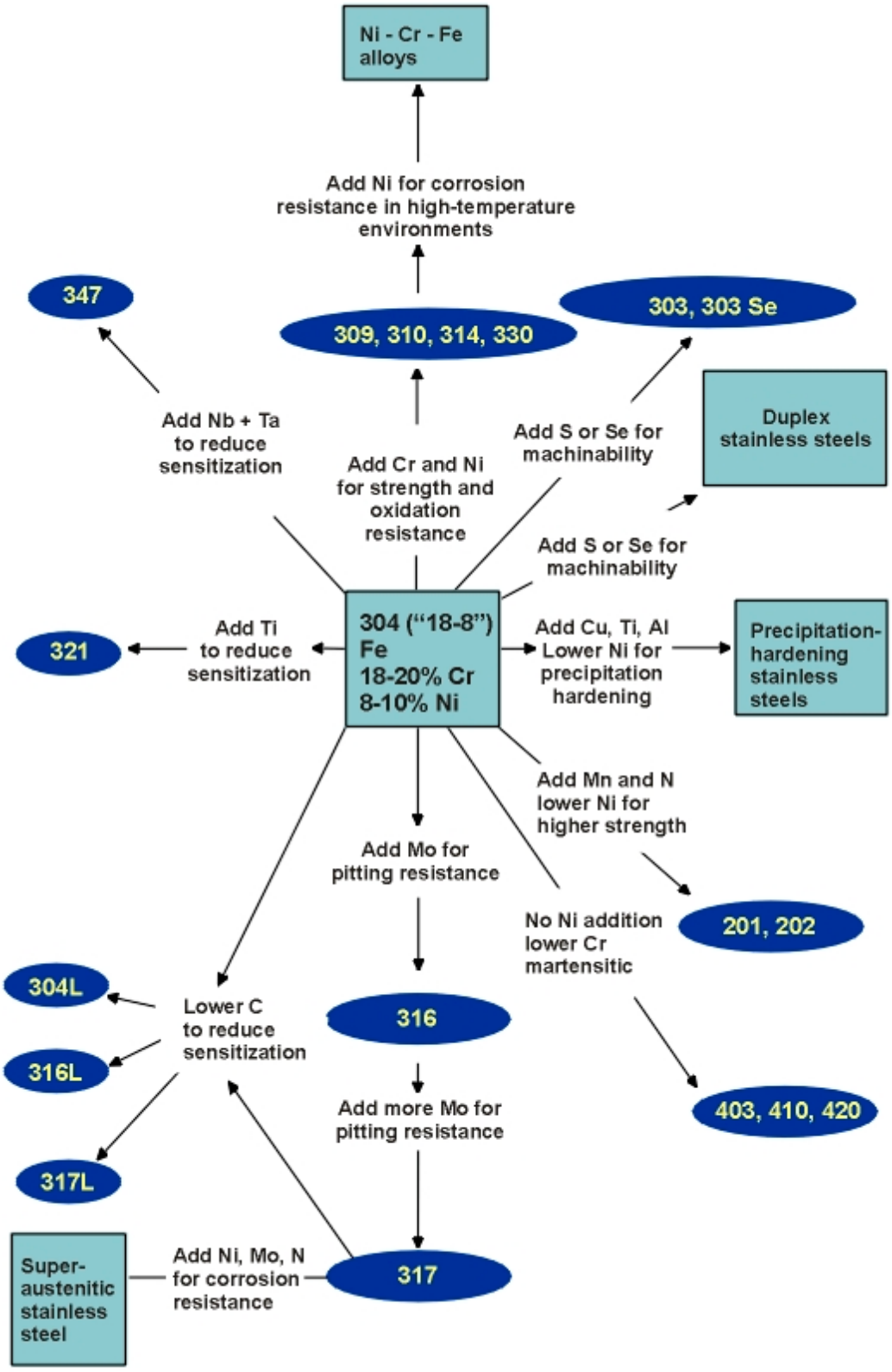

Figure 1.1 - Typical compositions of austenitic stainless steels [3].

Fig. 1.2: Diagram of the new stainless steel bearings made from type 316 stainless steel to offer longer service life and increased corrosion resistance [6].
Fig. 1.3: Diagram of the Dyson twin drum, Contrarotator™ [7]. This concept allows clothes to be cleaned through increased fabric flexing thus allowing effective dirt release.

It shows that 8Ni wt% is enough to ensure that the alloy can become fully austenitic at a high temperature and can then be quenched to ambient temperature and retain all the austenite. To counteract this, nickel is added as an austenite stabiliser, so that the microstructure at ambient temperature is austenitic. Figure 1.4 [12] illustrates the region where stable austenite forms within a pure Fe-18Cr wt% alloy. It shows that 8Ni wt% is enough to ensure that the alloy can become fully austenitic at a high temperature and can then be quenched to ambient temperature and retain all the austenite.

Attempts have been made to reduce the nickel content, as this is a relatively expensive alloying element. Alternatives include increasing amounts of nitrogen and manganese. There is also a demand for zero-nickel steel, as many people believe they can develop nickel allergies [13]. This can occur when they come into contact with everyday items such as jewellery and kitchen utensils.

Recently, Wang [14] conducted studies on the effect of yttrium in type 304 stainless steels. It was found that its high oxygen affinity helped contribute to the passivity of the surface oxide layer, already provided by chromium. Moreover, experimentation showed that the mechanical

properties of the surface oxide were also enhanced. The result was improved corrosion and corrosive wear resistance.

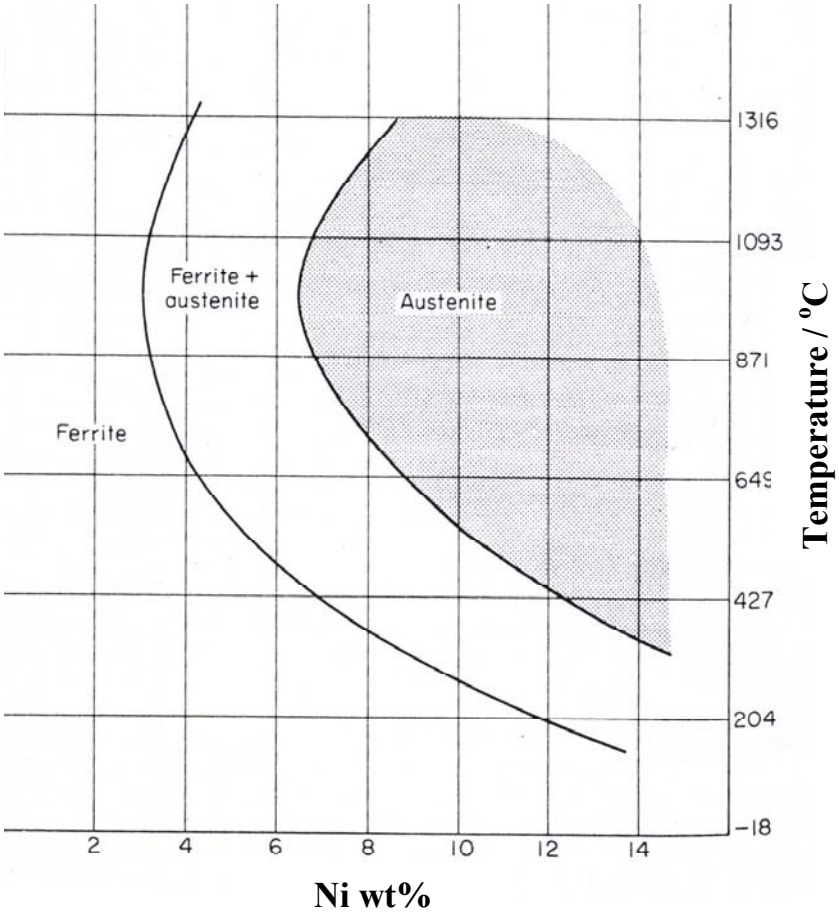

Figure 1.4: Shows the relative stability of austenite with varying amounts of nickel at different temperatures with Fe-18Cr wt% [12].

1.2 Martensite formation

Nickel not only stabilises austenite relative to ferrite, but it also reduces the martensite-start (M_s) temperature (figure 1.5) [7]. For austenitic stainless steels of the type discussed here, it is required to depress the M_s temperature below ambient (298 K). Martensite can also be induced by plastic deformation. The temperature M_d below which strain-induced martensite [16] forms is generally higher than M_s; nickel suppresses M_d.

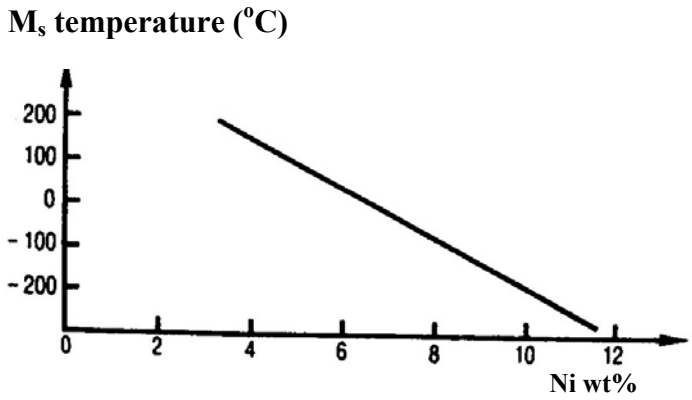

Figure 1.5: Martensite start (M_s) temperature plotted against nickel content for 18Cr wt% - 0.04C wt% steel [5]. The M_s temperature goes down to -273^{o}C, thus making it impossible to induce martensite.

However, the use of carbide forming elements such as titanium can promote martensite because they remove carbon from solid solution and may themselves stabilise ferrite. [5,17].

2. Tensile tests

Tensile tests are used to characterise the elastic and plastic deformation of materials [18]. They are a good measure of their behaviour during statically applied stresses. A parallel-sided sample of predetermined dimensions is pulled to the point of fracture (figure 2.1), whilst monitoring load and elongation.

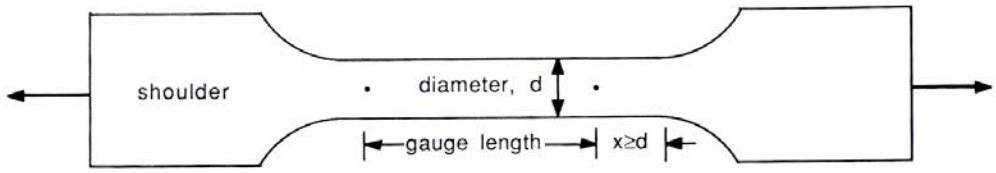

Figure 2.1 – Diagram of a typical tensile specimen [12].

A typical engineering stress-strain curve can be seen in figure 2.2. In many materials, yielding is gradual so that the elastic limit is ill-defined. Instead, a proof stress is universally identifiable as the stress corresponding to a plastic strain of 0.002.

As plastic deformation dominates and continues, the shear stress also increases, a phenomenon called work hardening. However a maximum engineering stress, the ultimate tensile strength [20], is achieved because of the onset of local non-uniform deformation. At this point of zero slope, the increase in load from work hardening is equal to the decrease in load experienced from area reduction. This contraction continues as the load increases further, as the ability to cause added strain is lower in this region, therefore 'necking' results [12].

The engineering stress, based on the original cross-sectional area of a test sample, is appropriate to find the UTS as it defines the maximum load that can be supported. True stress and strain, as seen in figure 2.2, increase throughout deformation because they are calculated using instantaneous dimensions.

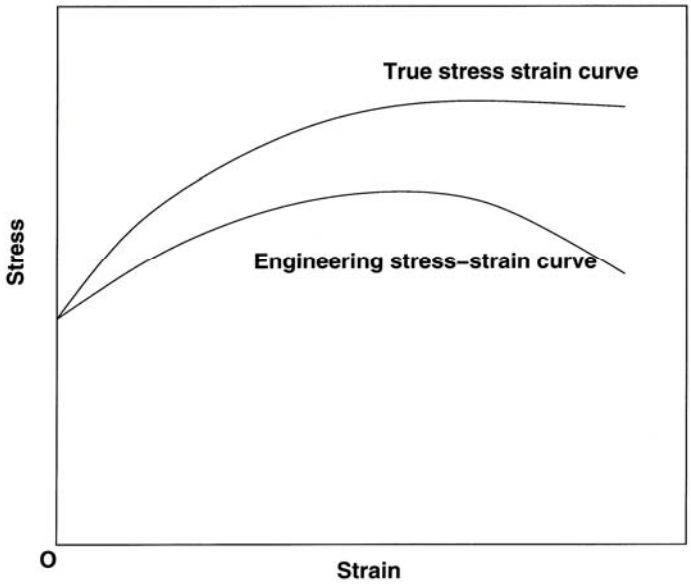

Figure 2.2 - Stress-strain curve showing the difference in curvature between the engineering stress and true stress.

To account for area changes, the instantaneous load F per unit of actual area A is found for true stress:

$$\sigma = \frac{F}{A} \tag{2.1}$$

Similarly, true strain gives a more accurate description of the change in length dL of a sample length L_o, in relation to its instantaneous length L:

$$\varepsilon = \ln \frac{L}{L_o} \tag{2.2}$$

This relation is important, as numerical values found for tension and subsequent compression would be identical, but have opposite signs.

True-stress strains can often be expressed by a power-law relationship for ductile metals [21]:

$$\sigma = K\varepsilon^n \tag{2.3}$$

where n is the strain hardening exponent and the gradient of the curve, K is the strength coefficient, and σ and ε are the true stress and true strain values respectively. The parameter n is generally used to characterise strain-hardening behaviour:

$$n = \frac{d(\ln\sigma)}{d(\ln\varepsilon)} = \frac{\varepsilon}{\sigma}\frac{d\sigma}{d\varepsilon} \tag{2.4}$$

3. Plastic Deformation in Crystalline Metals

Assume that austenitic stainless steel has a perfect lattice. If a plane of atoms slide over one another, this motion is called slip. These shear movements occur on defined crystallographic surfaces, called slip planes, and along specific slip directions.

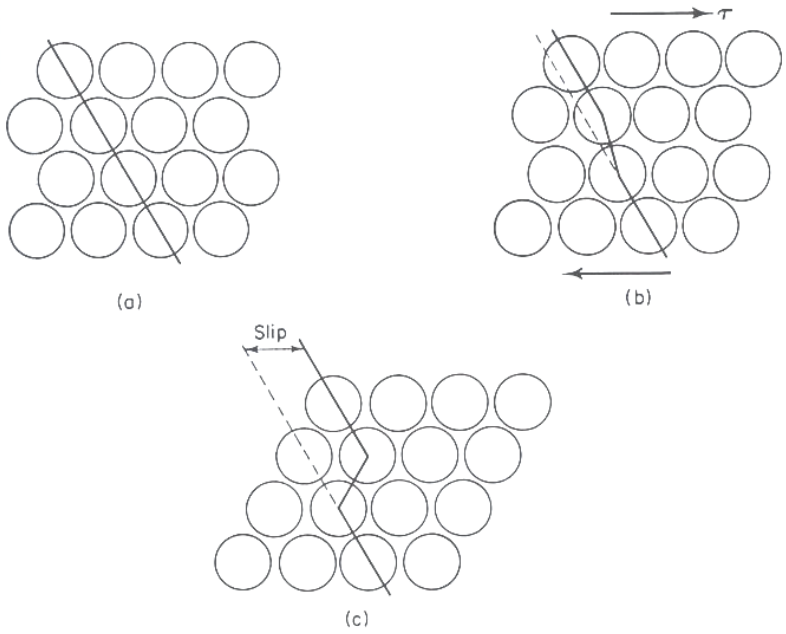

Figure 3.1(a) show the positions of atoms before slip; (b) shows the process of slip when a shear stress τ is applied; (c) is the atoms residing in their new configurations without the applied stress, hence signifying plastic deformation [12].

As shown in figure 3.1, the atoms lie in new positions after slip [12]. However, an equilibrium position can be re-established so that no stress is required to hold them. Hence as the load is released, the atoms do not return to their original positions, so it is regarded as plastic deformation.

However, the theoretical stresses for slip in a perfect steel is much greater than in practice [19]. This indicates that imperfections must be present within metallic crystals. To be significant, they have to provide a slip mechanism and be able to reduce the strength of steels by several orders of magnitude.

Austenitic steels have a face-centred cubic (fcc) lattice [19]. The shortest lattice vector is from one corner of the cube to the nearest face centre. As deformation usually operates on a plane where there is close atomic packing, slip occurs on $\{1\bar{1}1\}$ planes in <110> directions. In fcc metals, there are twelve slip systems in total, as the {111} planes have four different orientations.

3.1 Dislocations

Dislocations are common defects in steels, which are responsible for the majority of plastic deformation within metals [19]. Their slip direction is described in terms of Burgers vectors, corresponding to a closure failure of a Burgers circuit (figure 3.2). If the lattice is perfect, a closed rectangular loop will result and no failure in the circuit. However, a closure failure occurs if a dislocation is present. The magnitude and direction of this error therefore defines the Burgers vector, *b*.

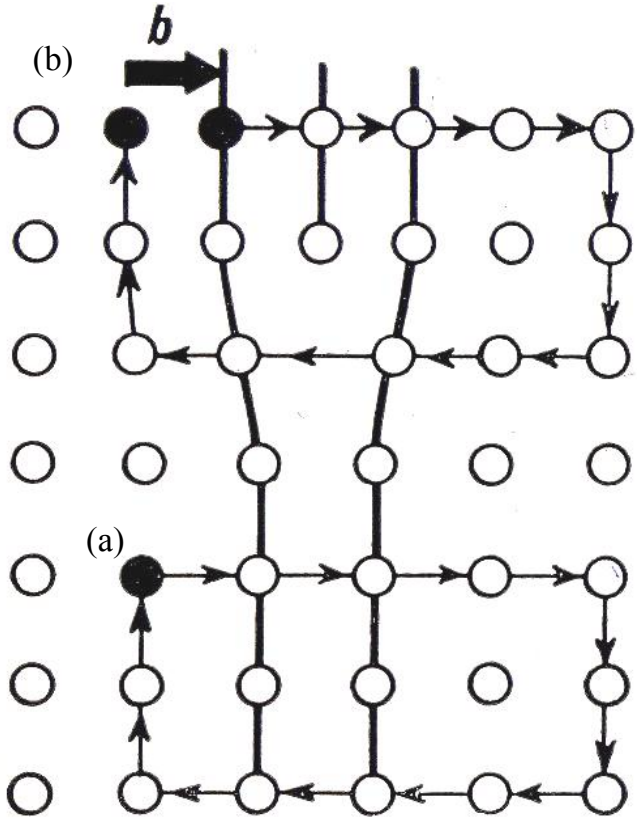

Figure 3.2 describes two Burgers circuits: (a) in a perfect crystal and (b), an imperfect lattice where there is a closure failure in the presence of a dislocation [19].

Dislocations allow slip to be localised so that the stress required for plastic deformation is greatly reduced when compared to the wholesale sliding of planes over one another. Inhibiting their motion can therefore increase the strength.

3.1.1 Edge dislocations

Figure 3.3 is a simple 2D representation of a perfect lattice. Here, all the bonds would need to be broken at once for slip. By contrast, in figure 3.4, the presence of a dislocation means that slip happens in a piecewise manner. Hence only a few bonds have to be broken at any instance, thus requiring a smaller stress for slip to progress [12].

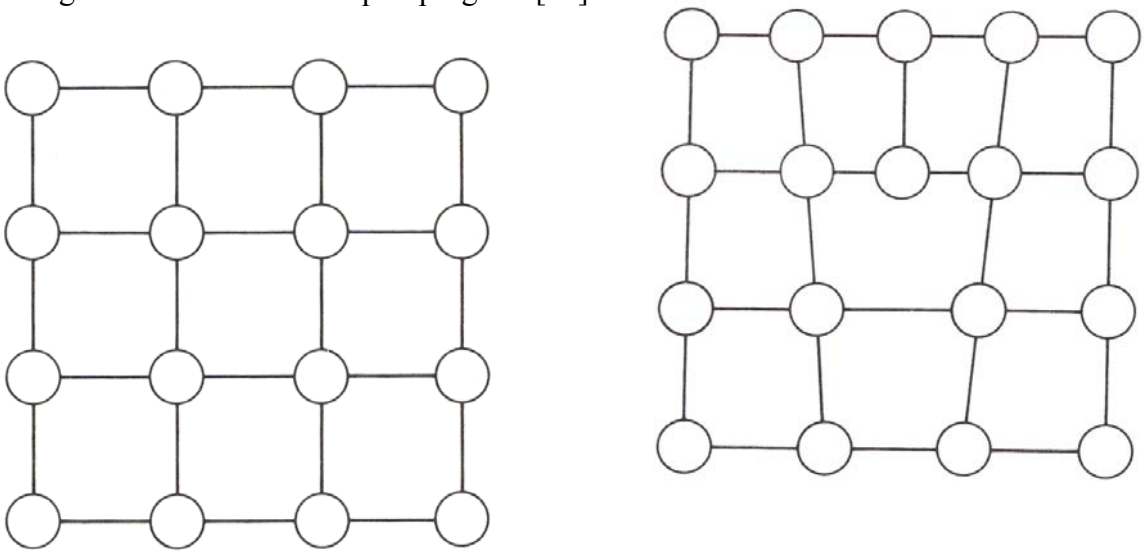

Figure 3.3 is a perfect 2D lattice, whereas figure 3.4 includes an extra plane of atoms, hence causing the introduction of an edge dislocation [12].

The region of atomic irregularity is described by the line along the lower edge of the plane ending within the crystal. This line describes an ‘edge’ dislocation. An analogy is a hump in a carpet, which can move from one side to the other whilst moving the carpet by only a small fraction. The forces resisting motion are therefore easily overcome by a small fraction of their area, when compared to a perfect lattice structure. Slip is normally parallel to the shear stress direction, which means that edge dislocations are usually confined to their current slip plane.

However, non-conservative movement is required [19] if they want to move above or below their slip plane. This involves the removal of the extra half plane of atoms away from the dislocation by diffusion, also known as “climb”, which requires thermal activation.

3.1.2 Screw dislocations

These are similar to edge dislocations, as they both cause atomic discontinuity. However, this interruption is not caused by extra atomic planes, but by the generation of a helicoid distortion instead. Figure 3.5 illustrates the geometry, where a plane of atoms along a dislocation path finish on a different plane than it initially began on. The slip direction is perpendicular to the shear stress, but parallel to the screw dislocation line. This means that any plane that cuts through a dislocation will have a Burgers vector and hence a slip plane, which allows slip on multiple planes.

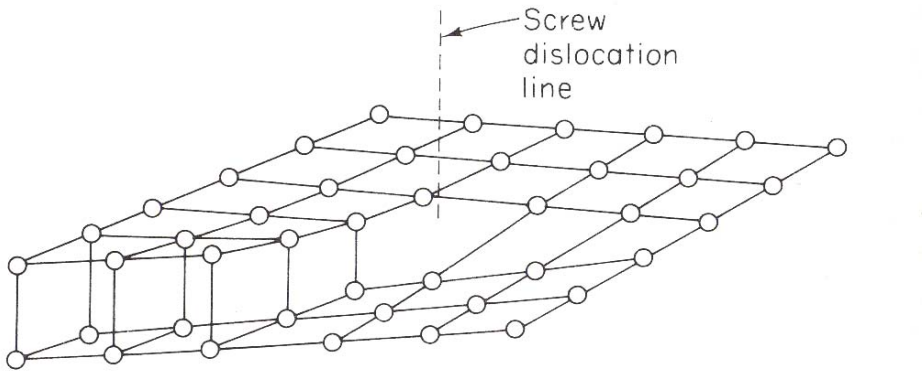

Figure 3.5 shows a screw dislocation in a simple cubic lattice [12].

Figure 3.6 shows this “cross-slip” event. It shows that screw dislocations can alter direction from shear stress changes caused by obstacles or other dislocations. This mechanism is particularly important for ductile metals, as more plastic deformation and barrier bypassing is allowed, compared to edge dislocations. There is little thermal activation required for this process; only high stresses [22].

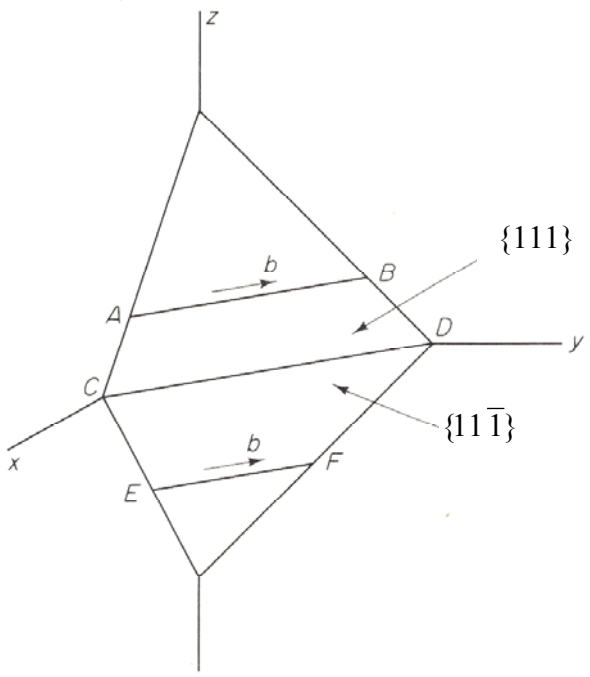

Figure 3.6 shows multiple planes where cross slip of a screw dislocation can occur on an fcc crystal. The dislocation AB moves along the {111} plane towards C and slips onto the {11 $\bar{1}$} plane towards EF [12].

3.2 Stacking faults

Within fcc metals, close-packed atom layers are stacked in ordered ABCABCABC sequences. However, the sequence can occasionally contain errors, often produced by the dissociation of a unit dislocation into two imperfect dislocations. This occurs to minimise the overall defect energy. Stacking layers can, for example, change to ABCACABCA, and therefore create a stacking fault [23]. This process is well-illustrated in figure 3.7.

If the dislocations slip along vector b_1, the atoms in the *B* position move across to *B* positions again, hence preserving the stacking sequence. However, if it energetically favourable, then slip may occur along vector b_2 to the *C* position, creating a partial dislocation:

$$\frac{a}{2}[10\bar{1}] \longrightarrow \frac{a}{6}[2\bar{1}\,\bar{1}] + \frac{a}{6}[11\bar{2}] \qquad (3.1)$$

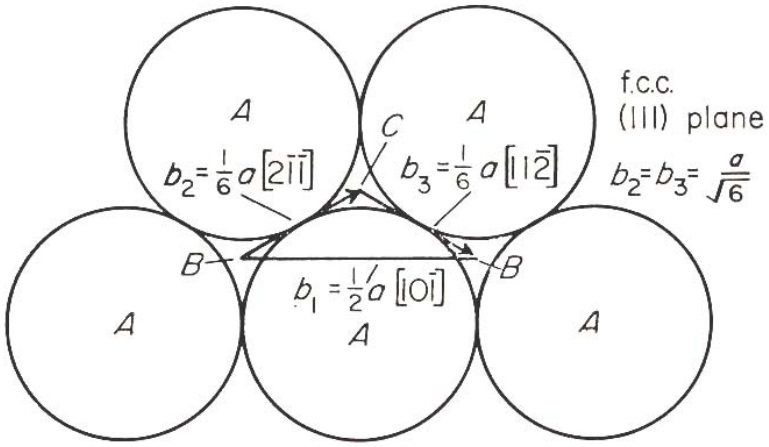

Figure 3.7 shows the dissociation of a dislocation into partials in a fcc lattice [19].

The region between the pair of partials is a stacking fault. As the energy of the dislocation is proportional to the square of the Burgers vector, it is clear that the dissociation lowers the energy and becomes favourable as long as the fault energy is not prohibitive. In austenite, both intrinsic and extrinsic faults are possible. The former describes a missing layer, ABCBCA, and the latter an extra layer, ABCBABC.

The fault is described as a narrow hexagonal close-packed (hcp) zone bound by partial dislocations. These partial dislocations have parallel components in their Burgers vectors. The parallel components repel each other, whereas the stacking fault energy (SFE) involved tend to attract the partials.

The equilibrium width d_o of the stacking fault increases as its energy decreases [18], which can be found by using:

$$d_o = Gb^2 \Big/ 2\pi(1-\nu)\gamma \qquad (3.2)$$

where γ is the SFE, G is the shear modulus in the glide plane, ν is the Poisson's ratio and b is the Burgers vector of both partial dislocations.

Typical SFE values are in table 3.1, which indicates that composition [24] is an important variable [15,25]. High concentrations of manganese and nitrogen typically reduce the SFE of austenite. However, an increase in temperature has the opposite effect by constricting the fault [19], hence raising the SFE [25,26]. Overall, low values of SFE increase the width of stacking faults. This effectively increases the work hardening rate as it is harder for dislocations to cross-slip; the UTS is therefore increased [19].

Metal	***Stacking Fault Energy*** / 10^{-3} J m^{-2}
303 Stainless Steel	8
304 Stainless Steel	20
310 Stainless Steel	45
Silver	25
Gold	50
Copper	80
Nickel	150
Aluminium	200

Table 3.1 Typical values of stacking fault energy [18].

3.3 Jogs

Dislocations on different planes may intersect with each other during plastic deformation. The result is the formation of 'jogs', which increase the length and energy in one or both of the dislocations. This intersection may change the character of the jogged dislocations, and hence reduce mobility.

A more rigorous analysis can be found in [19], but jogs and dislocations always have equivalent Burgers vectors, so they move together freely. However, when screw dislocations interact, the jogs require non-conservative movement (i.e. dislocation climb). The jogs then tend to become stationary and hence restrict dislocation movement. It is also suggested that jogs inhibit dislocations further by dissociating into partial dislocations [19]. This may show that screw

dislocations are not as mobile. Nevertheless, they are still able to move along slip planes with common slip directions.

3.4 Grain size

This is a common strengthening technique employed in many steels. The relationship between grain size and strength was introduced by Hall and Petch [17,18,27], who related the yield stress, σ_y, to the grain size d:

$$\sigma_y = \sigma_o + k_y d^{-1/2} \qquad (3.3)$$

where σ_o is the friction stress contribution from the grain boundary, and k_y is a grain boundary hardening constant. Figure 3.8 shows the dependence of yield strength upon grain size. The parallel series on the graph shows that k_y is unaffected by temperature. It has also been found that this relationship is true, regardless of the crystal structure [28].

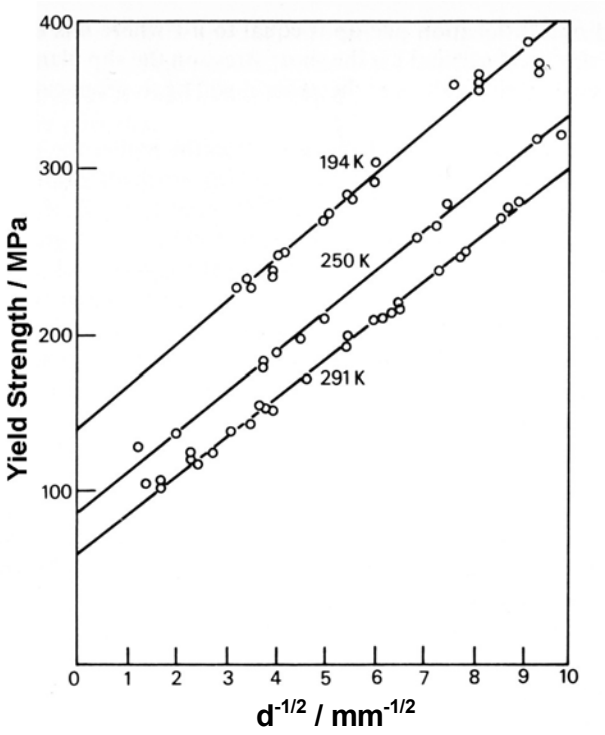

Figure 3.8 - Hall-Petch relationship of yield strength as a function of grain size (mild steel) [27].

Dislocations will encounter and pile-up at grain boundaries. Once a critical stress concentration has been achieved, sources are stimulated in adjacent grains leading to a propagation of plastic deformation.

Small grains involve fewer dislocations in the pile-ups and hence the applied stress has to be increased to cause yielding. This is due to the smaller distances involved [27], hence yield and ultimate tensile strength increase.

There is a variety of ways that an average grain size can be established. One method used in industry is one devised by the Japanese Standards Association [29].

They have a common measure called the grain size number, G_s:

$$m = 8 \times 2^{G_s} \tag{3.4}$$

where m is the number of grains mm^{-2} when viewed at a magnification of 100. As seen in table 3.2, a large G_s equates to a small grain size:

G_s	m
-3	1
-2	2
-1	4
0	8
1	16
2	32

Table 3.2 Typical values of G_s and m when using equation 3.4.

4. Hardening Mechanisms

4.1 Strain hardening

This occurs due to the pile-up and entanglement of dislocations, which in turn impedes their motion as deformation progresses [5]. The reorientation of grains during plastic straining can further increase the resistance to deformation [18]. As further strain is required, more stress is needed. However, when a critical stress is reached, they may pass through the grain boundary. A consequence is that the strain-hardening rate decreases.

Unfortunately, ductility is adversely affected by adopting this method. Austenitic steels have a higher hardening rate than ferritic alloys. As previously mentioned, a low SFE signifies a wide stacking fault, where cross-slip is difficult [15]. As the width increases, the resistance to motion through the lattice also increases. A high work-hardening rate would therefore result, naturally increasing tensile strength [2]. Compositional modifications therefore affect both the work hardening rate and SFE [25].

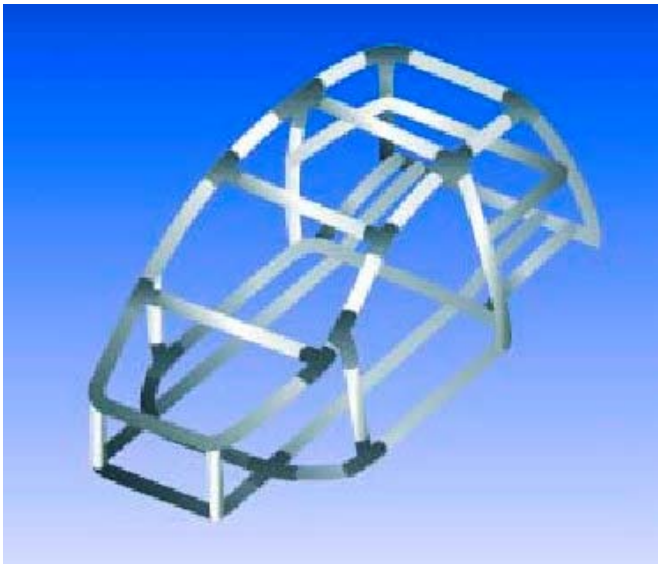

Figure 4.1 – Diagram of a stainless steel tubular space frame, designed for use in passenger cars [10].

For engineering applications, a ratio between yield strength and density, called specific strength, is sometimes used as a measure to compare different materials [10]. This is often the case for when strength and weight is a design concern; in car safety, for example. The use of strain

hardening can therefore offer austenitic stainless steel an increase in specific strength without increasing the weight. However, this ratio would be most useful when comparing different types of materials.

Austenitic stainless steels are also now being realised as viable alternatives to aluminium and high strength low alloy (HSLA) steels. They are especially useful for energy absorbing components, such as “space frames” for passenger cars, as shown in figure 4.1. This is because upon crash impact, the strain rate increases. However, the resistance to deformation also increases as a result, hence its usefulness.

4.2 Solid Solution Hardening

There are two kinds of solutions; interstitial and substitutional. The first describes small atoms that occupy the spaces between larger solvent atoms. Elements such as carbon, nitrogen and boron are interstitial due to their small size relative to iron. The hardening effect of each element is also related to its size, according to Hume-Rothery [19]. The ratio of the solute to the solvent atoms must be less than 0.59 for interstitial solutions [12].

The mechanism involves elastic distortions of the lattice, so that dislocation movement is impeded. As shown in figure 4.2, nitrogen atoms are squashed into the tiny interstitial spaces, where the resultant strain field interferes with the dislocation strain field. Although the amount of solute atoms is very low, this strain effect is not local but distributed throughout the lattice structure.

This interaction energy therefore raises the stress required to move dislocations, sometimes pinning them [5]. Carbon is a comparatively good solid solution hardener and gamma stabiliser, but high concentrations risk $M_{23}C_6$ precipitation. The "M" refers to metal atoms, particularly chromium. Nitrogen, however, acts to stabilise the solid solution by reducing the coarsening of $M_{23}C_6$ by lowering the diffusion rate of chromium and carbon [5,15,31].

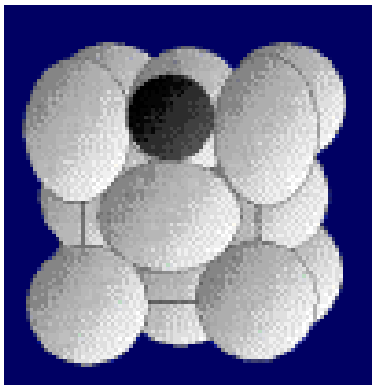

Figure 4.2 - Shows the distortion of an fcc-lattice due to the presence of an interstitial element [30].

Moreover, the presence of nitrogen during the annealing treatment inhibits ferrite transformation during cooling [32]. Because of this, nitrogen concentrations have been increased to the solubility limit [33]. To further extend this limit, manganese [1,13,33] and chromium [34] concentrations may also be increased.

Manganese should also be employed to nullify any effect on ductility from high nitrogen concentrations [17,35]. Well-designed high nitrogen steels are strong, ductile and free from martensite [5]. Without manganese, ductility and toughness are severely undermined by Cr_2N formation [31], especially at high operating temperatures [36].

For substitutional solution hardening, solvents atoms are themselves replaced by alternatives. These have a much higher solubility than interstitials. This is determined by similarities in crystal and electronic configurations, as well as atomic radius. Nevertheless, the lattice distortion effect, as with interstitials, again causes interference to dislocation motion, but not as great.

5. Precipitation

5.1 Chromium carbide formation

The precipitation of carbon in austenitic stainless steels can have detrimental consequences. To counteract this effect, such steels are annealed at around 1100^{o}C [5] and cooled rapidly to keep the carbon in solid solution. However, if the metal is kept within a critical temperature range (500-800^{o}C), either during slow cooling, welding or during service, $M_{23}C_6$ formation occurs. The precipitation takes place at grain boundaries, which consequently become surrounded by a chromium-depleted region, which becomes susceptible to intragranular corrosion [5]. Molybdenum can be partially substituted for chromium, as resistance to pitting corrosion is one of the main reasons for its addition to stainless steel [32]. However, it does hasten $M_{23}C_6$ formation through a reduction of solubility of carbon in austenite. The extent of substitution is therefore dependent on the holding temperature and its duration, as well as the quantity of carbon [17].

5.2 Stabilisation

A common practice employed to prevent chromium combining with carbon is to include strong carbide formers, which detract carbon from chromium. Transition elements are particularly potent MC carbide formers, such as titanium, niobium and vanadium. These stable carbides form during high temperature treatment instead of $M_{23}C_6$, figure 5.1. However, if this annealing process is prolonged, it could result in grain growth and decrease UTS [32].

The steel is first heated to a high temperature to dissolve precipitates and erase prior work hardening to achieve a solid solution. A rapid reduction in the temperature makes the solution supersaturated, causing precipitation of carbides or nitrides, which are not associated to intragranular corrosion. These finely dispersed *MX* carbides and nitrides impede dislocation movement [5] and also restrict grain growth [37].

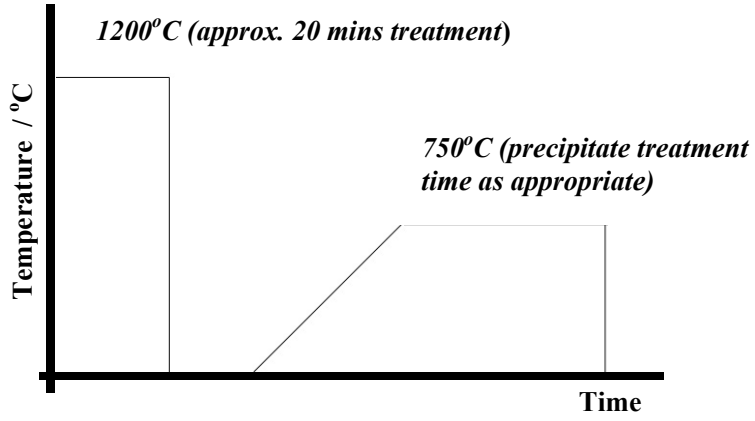

Figure 5.1 - Diagram of heat treatment for MC formation.

However, there are disadvantages with this procedure. The use of carbide-formers may lead to lower steel ductility [39]. Also, the hardening effect of carbon and nitrogen is reduced as they are taken out of solution [32]. Moreover, as the interstitials are austenite stabilising elements, their absence increases the risk of ferrite formation. Hence nickel concentrations are increased to compensate for this deficiency.

5.3 Precipitation Hardening Mechanism

Orowan determined the precipitation hardening mechanism as a function of interparticle spacing [12,19], and the movement of dislocations around these impediments. The required shear stress τ was shown to increase inversely with particle spacing f:

$$\tau = \frac{Gb}{f} \qquad (5.1)$$

Figure 5.2 shows Orowan's strengthening model with fine particles. The dislocations are quite free to move on their approach toward the particles. Hence they start to bend around them as they approach the obstacles (fig. 5.2(a)). However, for more strain in the metal to occur, the shear stress must increase.

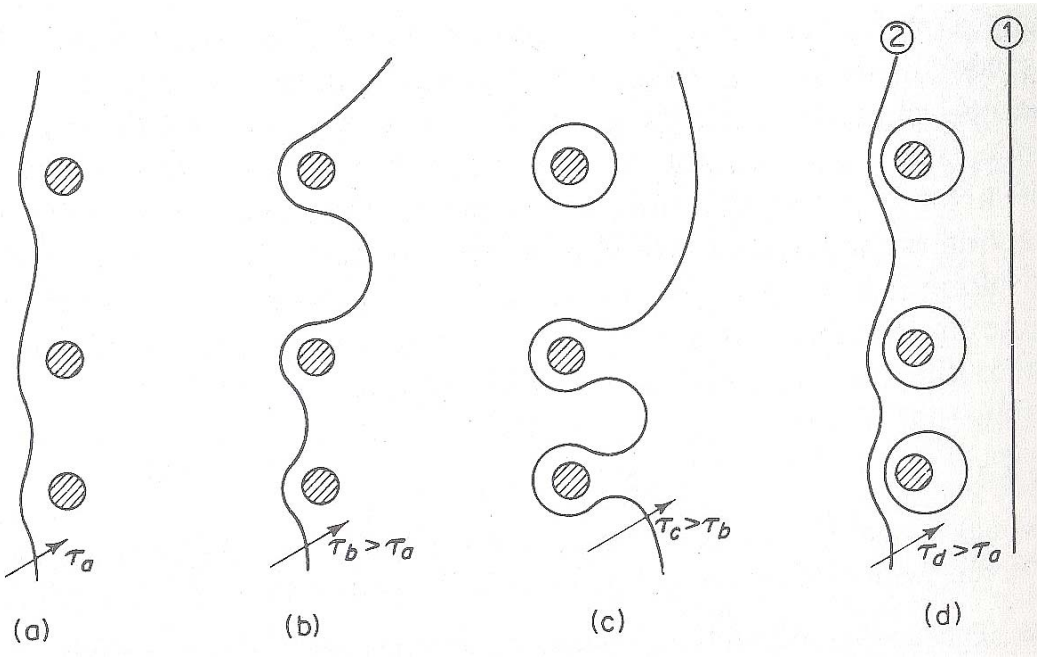

Figure 5.2 showing the Orowan strengthening model for when particles encounter dislocations in metals, where varying shear stress *(τ_a, τ_b, τ_c, τ_d)* is required for dislocation motion to progress [12].

Fig. 5.2(b) shows that initial stress increases allow the dislocations to bow between the particles. This can continue until the line completely wraps around the particle. Upon touching, the dislocation snaps away into a nearly complete straight line. However, a dislocation loop is left behind; a process that repeats and constructively forms secondary and tertiary loops (figs. 5.2(c) and 5.2(d)).

Note that figure 5.2(d) shows unimpeded motion, but in reality, particles would be continuously encountered.

The dislocation loops around the particles also produce a high strain strengthening effect, as they theoretically have a wider influence. This inevitably increases the stress required for dislocation motion through the lattice. However, there is a precipitate size and distribution issue. Particles smaller than 10 nm do not effectively stop dislocations, as thermal assistance allows them to easily bypass the obstacles. Likewise, precipitates dispersed greater than 1 micron apart allow dislocations to bow between them and hence dislocations easily pass through [22].

As previously mentioned, cross-slip by screw dislocations is a mechanism by which these obstacles can be bypassed. Here, the SFE could be lowered to introduce partial dislocations. As cross-slip would be restricted, the required stress and strain-hardening rate would undoubtedly increase. In contrast, high SFE metals would require lower stresses for motion. Nevertheless, dislocations would still elongate as a result of cross-slip, and become barriers for other dislocations [12], but resulting in a smaller increase in UTS.

5.3.1 Other elements in precipitation hardening

Boron and nitrogen both retard $M_{23}C_6$ formation by reducing the solubility of carbon in austenite [9]. However, boron has a particular use in nuclear power plants. It acts to absorb thermal neutrons generated from energy production, and $(FeCr)_2B$ precipitates form in austenitic stainless steel, producing a significant strengthening effect. However, as seen in figure 5.3, a loss of toughness and ductility makes it a tough compromise for the nuclear industry [21].

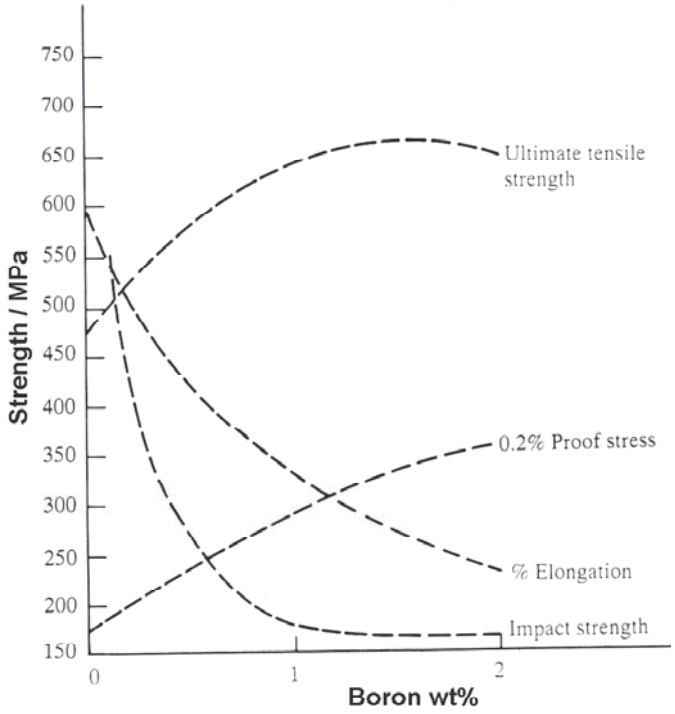

Figure 5.3 showing the influence of boron on the short term properties of type 304 stainless steel of composition 18Cr–10.3Ni–2.0Mn-0.03C-1.0Si wt% [38].

Phosphorus enhances strength [9], but it may embrittle the alloy and accelerate $M_{23}C_6$ precipitation [17], especially during a welding process. In spite of its brittle characteristics, it is often used to improve machinability [32]. It is also also be used with boron to produce fine carbide and nitride precipitation by trapping in vacancies and favouring precipitate nucleation [5].

Molybdenum is considered to be a good solid-solution hardener, and helps prevent pitting corrosion [11]. However, the nickel concentration has to be increased to enhance austenitic stability.

6. Intermetallic phases

As well as chromium-carbon interactions, there may be intermetallic phases produced, most of which are undesirable [16]. As an example, iron, nickel or manganese could be combined with chromium, titanium or vanadium [17]. There is a host of such phases recently reviewed in papers by Sourmail [39] and collaborative work between Padilha and Rios [16].

6.1 Sigma phase

This has a general composition, approximated to be $(Fe,Ni)_3(Cr,Mo)_2$ [16], which commonly precipitates on grain boundaries; it is associated with embrittlement [39]. To establish whether it precipitates, predictions based on electron configurations and the concentrations of alloying elements are required [5,17].

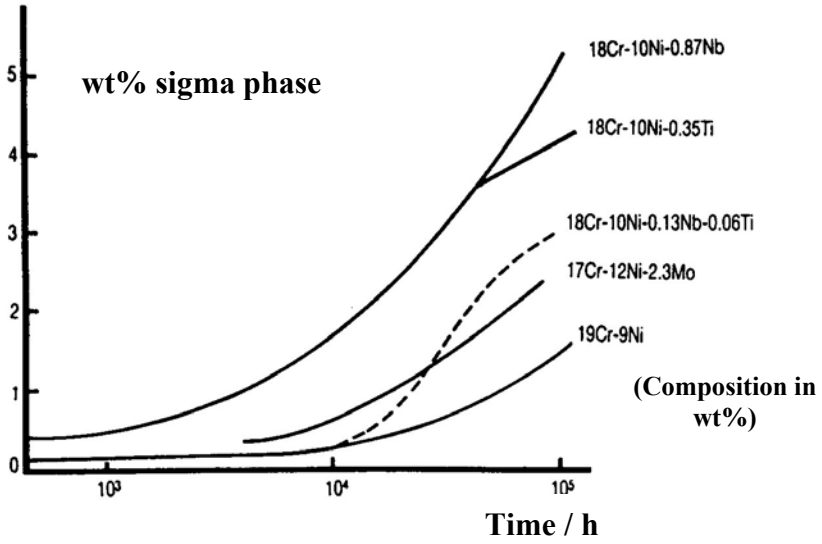

Figure 6.1 – Influence of alloying elements on sigma phase precipitation at 700°C [5].

Figure 6.1 shows how different alloys are susceptible to sigma phase formation. Elements such as molybdenum and niobium promote it, whereas nickel, carbon and cobalt hinder its development [16]. Figure 6.2 shows the role of carbon on sigma [5]. Large grains from high annealing temperatures create longer diffusion paths and hence mitigate the effects of sigma

phase [17]. The absence of delta-ferrite also restricts its formation, as the rate of growth in this phase is approximately one hundred times faster than in austenite [5].

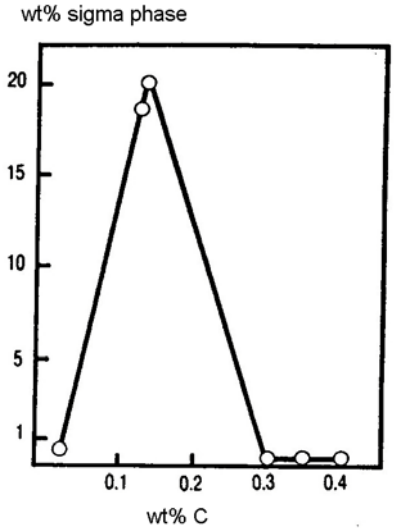

Figure 6.2 - Shows the various ranges where certain carbon values promote and challenge sigma phase precipitation for non-stabilised 25Cr – 20Ni wt% austenitic stainless steels [5].

6.2 Laves phase

In stable stainless steel grades, Fe_2Nb or Fe_2Ti typically form. Molybdenum can become a component element, especially with concentrations between 2-3 wt% [16] but only after long aging periods. Nevertheless, Laves phase is a minor constituent within the majority of stainless steels. There is evidence that Laves phase is brittle at room temperature; elements such as nickel and carbon help to suppress it [39]. Delta ferrite also counteracts Laves phase, but on the other hand it encourages sigma and chi phase formation.

6.3 Chi, G and Z phases

These phases tend to occur less frequently than those mentioned above. *G*-phase, as the name indicates, has a tendency to form on grain boundaries. Many phases form at boundaries but do not weaken. It weakens steel by lowering rupture strength and ductility [9]. Its composition

includes silicon, which is stabilised by transition elements. An empirical formula is $A_{16}D_6C_7$, where *A* is nickel, *D* is either niobium or titanium and *C* is normally a group four element such as carbon. As nickel is taken up by this phase, its concentration has to increase to ensure austenitic stability [39].

Chi is mostly found in type 316 and 321 stainless steels. Its empirical formula is $Fe_{36}Cr_{12}Mo_{10}$, and is thought to be similar to sigma [16]. However, this phase has considerable interstitial space to allow carbon to form $M_{18}C$, most commonly found on grain boundaries and dislocations. This is quite a rare phase, but it has a similar nature to the sigma phase [9] and is found at temperatures above 750^{o}C [39].

The *Z*-phase tends to form carbonitrides within niobium-based stainless steels where high nitrogen concentrations are found [39]. The reported formula is $Cr_2Nb_2N_2$. But if there is an excess of niobium, *NbC* is also present. This phase is commonly found as fine particle dispersions on grain boundaries, which makes it useful when seeking good creep properties for power plant steels [39].

7. Modelling of Tensile Properties

Many linear regression models have been produced [1,2], in an attempt to characterise the strength of steels, including 0.2% proof stress and UTS. There have been many variables described in this survey that, at least, have some influence on the final strength properties of austenitic stainless steels.

Because of the plethora of variables, it is necessary to capture the complex interactions in order to understand how strength is developed. As the effects may not be entirely linear, a non-linear approach is required to address this issue. Bhadeshia and MacKay have used neural networks to treat problems such as these [40]. Examples include estimating the mechanical properties of steel welds [41], hence this modelling technique may be useful to investigate the tensile properties of austenitic stainless steels.